Supplemental Information

Projected Increase in Extremely Active Atlantic Hurricane Seasons

*Hosmay Lopez[1], Sang-Ki Lee[1], Robert West[2,1], Dongmin Kim[3,1], Gregory R. Foltz[1], Ghassan J. Alaka, Jr.[1], and Hiroyuki Murakami[4]

[1]Atlantic Oceanographic and Meteorological Laboratory, NOAA, Miami, FL

[2]Northern Gulf Institute, Mississippi State University, Mississippi State, MS, USA

[3]Cooperative Institute for Marine and Atmospheric Studies, University of Miami, Miami, FL

[4]Geophysical Fluid Dynamics Laboratory, NOAA, Princeton, NJ

Included materials:

Tables S1, S2, and S3

Figures S1, S2, S3, and S4

Supplementary Table 1. Return period (years) of ACE and TC number for each of the four scenarios: early period (1970-1994), early period plus accounting for mean changes only, early period plus accounting for variance change only; and recent period (1995-2021). The return periods are obtained from the SGS distribution shown in Fig. 1 where the confidence intervals are quantified by generating 500 SGS distributions using a Markov model with predetermined parameters and random linear and non-linear noise constrained by observations. See Methods.

	2005 season (active)		2014 season (inactive)	
	TC number = 28	ACE = 245	TC number = 8	ACE = 66.7
Early period	>1000	267±74	5±1	3±1
Early period + mean	114±25	63±20	>1000	11±2
Early period + variance	51±7	53±15	3±1	2±1
Recent period	16±2	23±3	24±7	6±1

Supplementary Table 2. HighResMIP. A total of 24 models (48 ensembles) for the TRACK and 16 models (39 ensembles) for the TempestExtremes algorithm are analyzed, totaling 87 ensembles. The X symbol indicates the model used and the numbers in parentheses the number of ensembles for each model.

Model (number of ensembles)		Atmosphere Resolution	TRACK	TempestExt	Reference
CMCC-CM2-HR4	(1)	100 km	X		Cherchi et al. 2019
CMCC-CM2-HR4_highresSST	(1)	100 km	X		Cherchi et al. 2019
CMCC-CM2-VHR4	(1)	25 km	X		Cherchi et al. 2019
CMCC-CM2-VHR4_highresSST	(1)	25 km	X		Cherchi et al. 2019
CNRM-CM6-1_highres	(1)	100 km	X	X	Voldoire, 2019
CNRM-CM6-1_highresSST	(1)	100 km	X	X	Voldoire, 2019
CNRM-CM6-1-HR_highres	(1)	35 km	X	X	Voldoire, 2019
CNRM-CM6-1-HR_highresSST	(1)	35 km	X	X	Voldoire, 2019
EC-Earth3P	(2)	100 km	X	X	Haarsma et al. 2020
EC-Earth3P_highresSST	(3)	100 km	X	X	Haarsma et al. 2020
EC-Earth3P-HR	(2)	50 km	X	X	Haarsma et al. 2020
EC-Earth3P-HR_highresSST	(3)	50 km	X	X	Haarsma et al. 2020
HadGEM3-GC31-LL	(5)	250 km	X	X	Roberts et al. 2019
HadGEM3-GC31-HH	(1)	50 km	X	X	Roberts et al. 2019
HadGEM3-GC31-HM	(3)	50 km	X	X	Roberts et al. 2019
HadGEM3-GC31-HM_highresSST	(3)	50 km	X	X	Roberts et al. 2019
HadGEM3-GC31-LM_highresSST	(5)	250 km	X	X	Roberts et al. 2019
HadGEM3-GC31-MH	(1)	100 km	X	X	Roberts et al. 2019
HadGEM3-GC31-MM	(5)	100 km	X	X	Roberts et al. 2019
HadGEM3-GC31-MM_highresSST	(3)	100 km	X	X	Roberts et al. 2019
MPI-ESM1-2-HR	(1)	100 km	X		von Storch et al., 2017
MPI-ESM1-2-HR_highresSST	(1)	100 km	X		von Storch et al., 2017
MPI-ESM1-2-XR	(1)	50 km	X		von Storch et al., 2017
MPI-ESM1-2-XR_highresSST	(1)	50 km	X		von Storch et al., 2017

Reference for HighResMIP models

Cherchi, A., Fogli, P. G., Lovato, T., Peano, D., Iovino, D., Gualdi, S., et al. (2019). Global mean climate and main patterns of variability in the CMCC-CM2 coupled model. Journal of Advances in Modeling Earth Systems, 11, 185–209. https://doi.org/10.1029/2018MS001369

Haarsma, R. J., Acosta, M., Bakhshi, R., et al. (2020). HighResMIP versions of EC-Earth: EC-Earth3P and EC-Earth3P-HR. Description, model performance, data handling and validation. Geoscientific Model Development. https://doi.org/10.5194/gmd-2019-350

Roberts, M. J., Baker, A., Blockley, E. W., Calvert, D., Coward, A., Hewitt, H. T., ... & Vidale, P. L. (2019). Description of the resolution hierarchy of the global coupled HadGEM3-GC3. 1 model as used in CMIP6 HighResMIP experiments. *Geoscientific Model Development*, *12*(12), 4999-5028.

Voldoire, A. (2019). CNRM-CERFACS CNRM-CM6-1 model output prepared for CMIP6 HighResMIP. https://doi.org/10.22033/ESGF/ CMIP6.1925

von Storch, J.-S., and Coauthors, 2017a: MPI-M MPI-ESM1.2-HR model output prepared for CMIP6 HighResMIP. Earth System Grid Federation, accessed August 2019, https://doi.org/10.22033/ESGF/CMIP6.762.

Supplementary Table 3. Climate models used in the study. All models were analyzed using a single ensemble member each for the historical and SSP585 emission scenarios from CMIP6.

Model Name	Institution
ACCESS-CM2	Australian Community Climate and Earth System Simulator (ACCESS)
ACCESS-ESM1.5	Australian Community Climate and Earth System Simulator (ACCESS)
CAMS-CSM1-0	Chinese Academy of Meteorological Sciences (CAMS)
CanESM5	Canadian Centre for Climate Modeling and Analysis (CCCma)
CESM2	National Center for Atmospheric Research (NCAR)
CESM2-WACCM	National Center for Atmospheric Research (NCAR)
EC-Earth3	European Consortium (EC)
EC-Earth3-Veg	European Consortium (EC)
GFDL-CM4	Geophysical Fluid Dynamics Laboratory (NOAA/GFDL)
GFDL-ESM4	Geophysical Fluid Dynamics Laboratory (NOAA/GFDL)
HadGM3-GC31-LL	Met Office Hadley Centre (MOHC)
MIROC6	Atmosphere and Ocean Research Institute (University of Tokyo), National Institute for Environmental Studies, and Japan Agency for Marine-Earth Science and Technology (MIROC)
MIROC-ES2L	Atmosphere and Ocean Research Institute (University of Tokyo), National Institute for Environmental Studies, and Japan Agency for Marine-Earth Science and Technology (MIROC)
MPI-ESM1.2-LR	Max Planck Institute for Meteorology (MPI-M)
MRI-ESM2.0	Meteorological Research Institute (MRI)
NorESM2-LL	Bjerknes Centre for Climate Research (BCCR)

Analysis of the representation of TC activity in HighResMIP versus Observations

Please note that the HighResMIP models chosen here are those that have made historical and future projections available under the SSP585 scenario (at the moment of this writing). Note that the SSP585 scenario is the only future scenario available in HighResMIP.

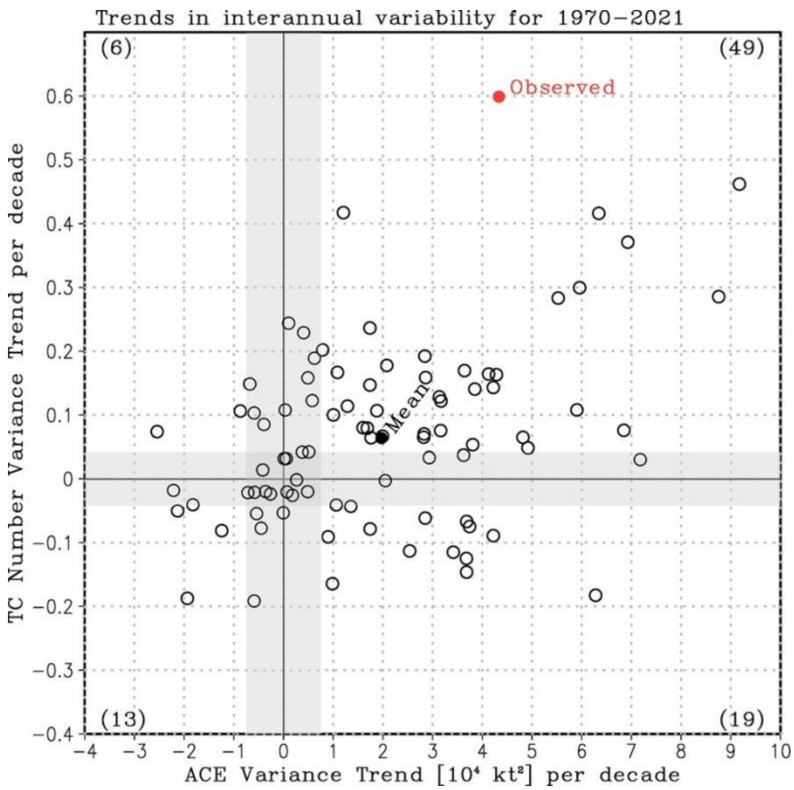

Supplementary Figure 1. Scatter diagram showing the interannual variability trends for ACE (abscissa) and TC number (ordinate) for the observed (red) and each of the 87 model ensembles from HighResMIP (open circles) for the period of 1970-2021. The ensemble mean is shown by a solid black circle. Trends inside the shaded gray regions straddling the zero axes are not significant at the 95% confidence interval. Numeric values in each corner represent the number of ensembles in each respective quadrant.

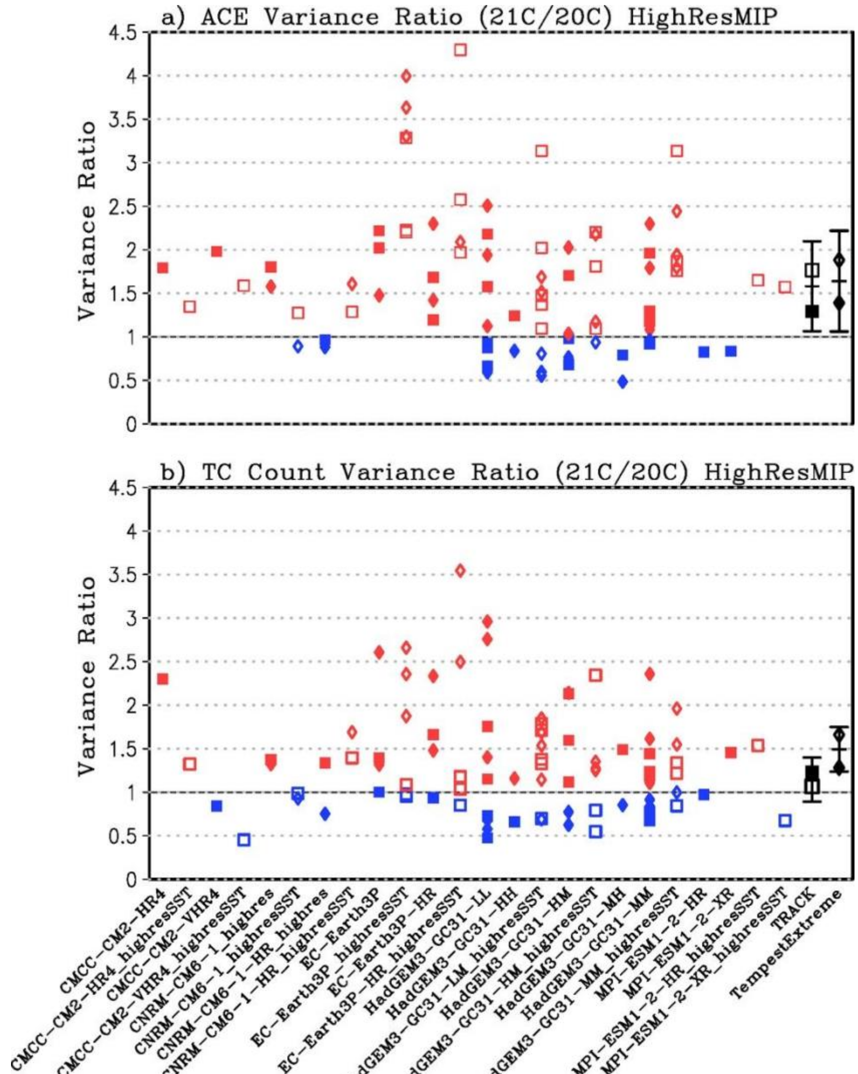

Supplementary Figure 2. Direct simulation of Atlantic TC activity changes. Interannual variability changes as measured by the 21C to 20C variance ratio from June-November for a) ACE and b) TC count from 24 models from the High-Resolution Model Intercomparison Project (HighResMIP). Two different TC detection methods are shown, TRACK algorithm (closed square) and TempestExtreme algorithm (closed diamond). Models with larger (smaller) 21C variance than 20C are shown in red (blue). Coupled (uncoupled) models are shown by solid (open) marks. The ensemble mean for each of the two detection methods are shown at the far right in black along with confidence intervals at a 95% level based on a bootstrapping technique (see Methods).

Supplementary Figure S3 shows spatial distribution of TC activity measured by storm transit per year per 5-degree box. To compare the models in a more quantitative way, we use a Taylor diagram, as shown in Supplementary Fig. 4. The Taylor diagram relies on statistical quantities that are closely related among each other as described in eq. S1 below. Here, obs (model) is the spatial pattern of observed (modeled) TC activity. RMSE is the root mean square error between the observed and modeled TC activity, (σ) is the observed (modeled) standard deviation, and cor is the anomaly correlation between observed and modeled TC activity.

$$[RMSE(obs, model)]^2 = \sigma_{obs}^2 + \sigma_{model}^2 - 2\sigma_{obs}\sigma_{model}cor(obs, model) \qquad eq.S1$$

From Supplementary Fig. 4, it is observed that the ensemble mean of HighResMIP models have a high spatial correlation (r=0.9) and an RMSE=0.47σ for TRACK and 0.55σ for TempestExtremes with respect to the observed TC spatial pattern of TC interannual variability, all well within the skillful range (i.e., smaller than the saturation RMSE value).

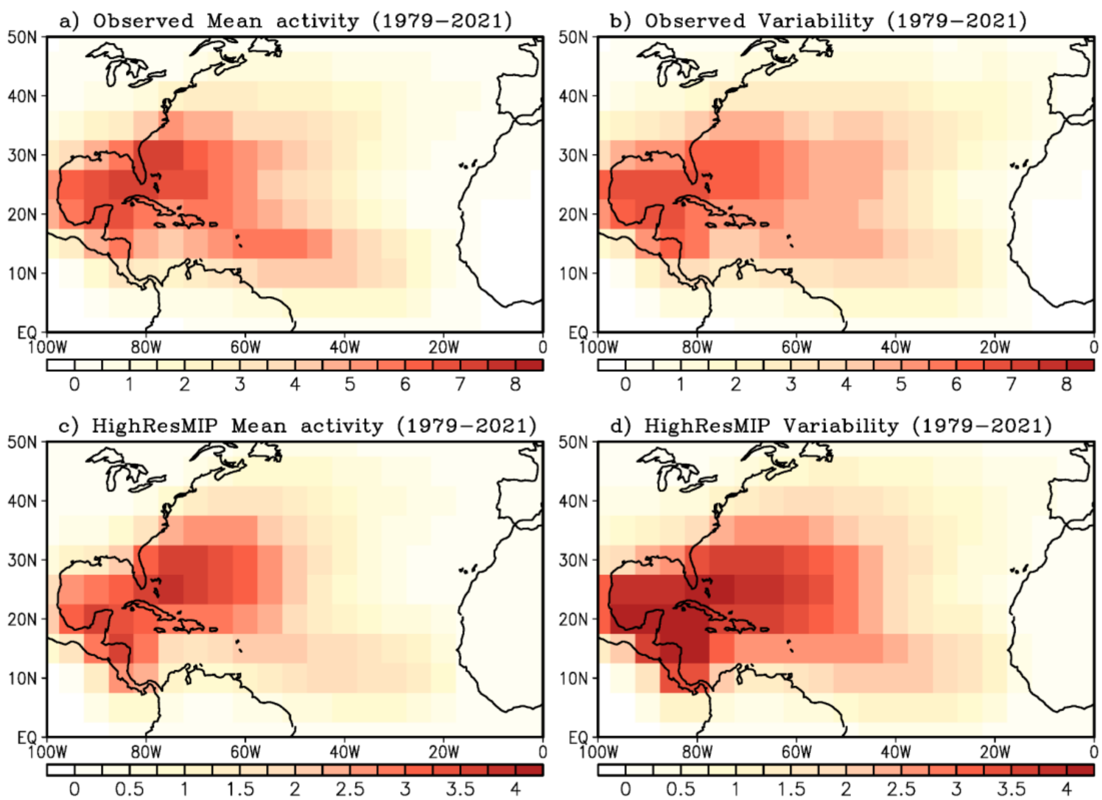

Supplementary Figure 3. Spatial distribution of tropical cyclone track density (storm transit per 5-degree latitude-longitude box per year). a) Observed track density and b) interannual variability for the 1979-2021 period. Similarly, c) and d) show track density and interannual variability from the ensemble mean from the HighResMIP models using both tracking algorithms (see Methods). Note that the color scale is different from the observed and HighResMIP for easier comparison.

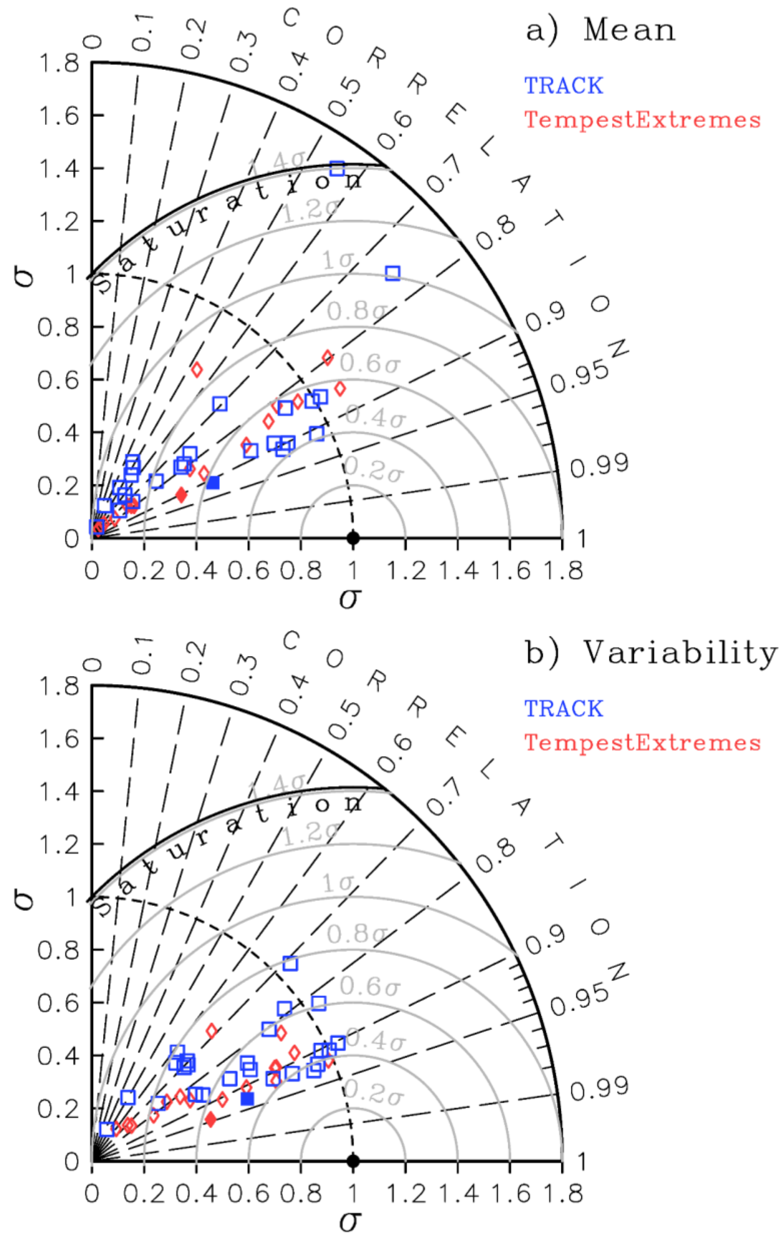

Supplementary Figure 4. Quality assessment of HighResMIP models in reproducing the observed spatial pattern of tropical cyclone track density for a) mean activity and b) interannual variability. Taylor diagram compares the standard deviation (radial axis) and spatial correlation (azimuthal axis) between the observed (i.e. HURDAT2, black circle) and HighResMIP modeled TC for the 1979-2021 period from TRACK (blue squares) and TempestExtremes (red diamonds) tracking algorithms. The ensemble means are shown by the solid marks where each model is shown by the open marks. The concentric semicircles centered at HURDAT2 represent the root mean squared error (RMSE) in standard deviation (sigma) units. Note that the RMSE and sigma are all standardized based on the HURDAT2 standard deviation, to facilitate comparison among different models.